

Fig. S1 The structure diagram of home-made instrument for detecting shrink force and peeling force. 1–lifting system; 2–pull/push dynamometer; 3–universal adjustable sample clamp; 4–temperature control system; 5–control panel.

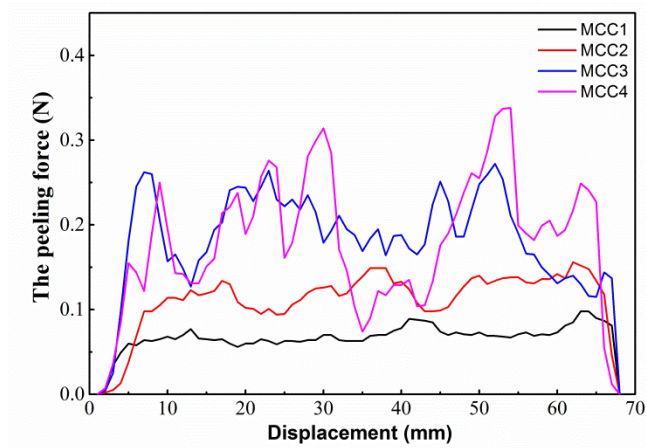


Fig. S2 Typical peeling force curves against displacement of various MCCs.

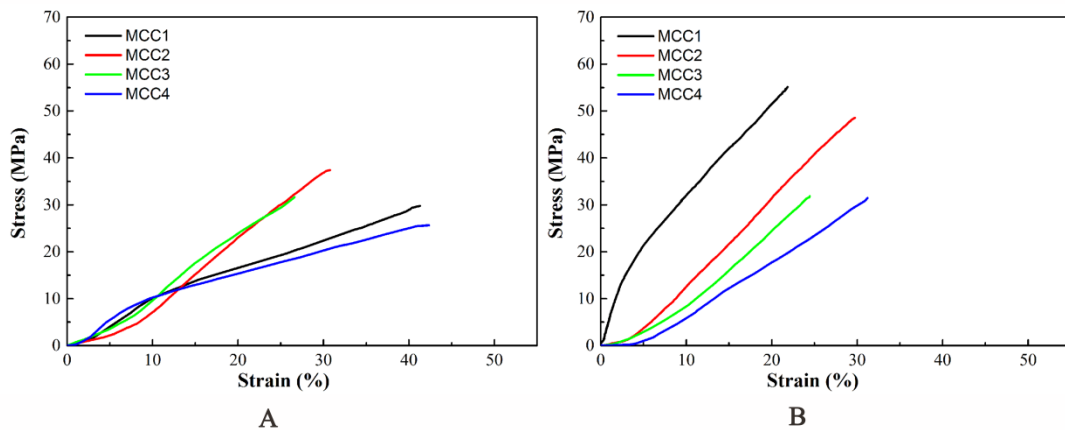


Fig. S3 Typical radial (A) and axial (B) stress-strain curves of various MCCs.

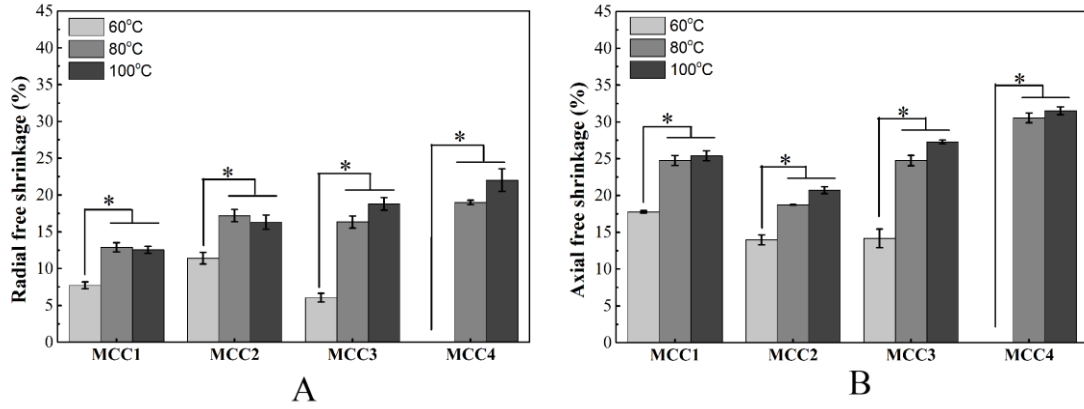


Fig. S4 The free radial (A,  $S_r$ ) and axial (B,  $S_a$ ) shrinkage of MCCs in water at various temperatures (60 °C, 80 °C, 100 °C). The data are expressed as the means  $\pm$  SEM ( $n = 15$ ), \* denoted  $p < 0.05$ .

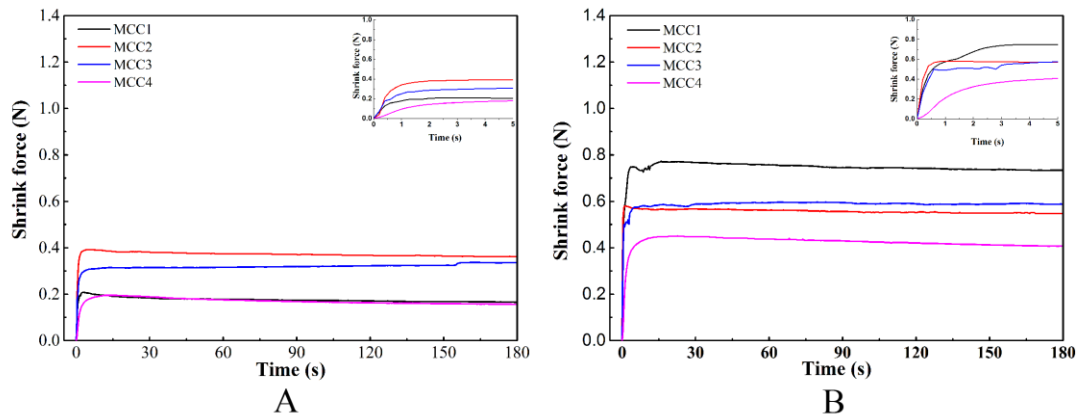


Fig. S5 Typical radial (A) and axial (B) shrink force curves against time of various MCCs in hot water at 80 °C. The corresponding partial enlarged curves within 5s were inset in the top-right corner.

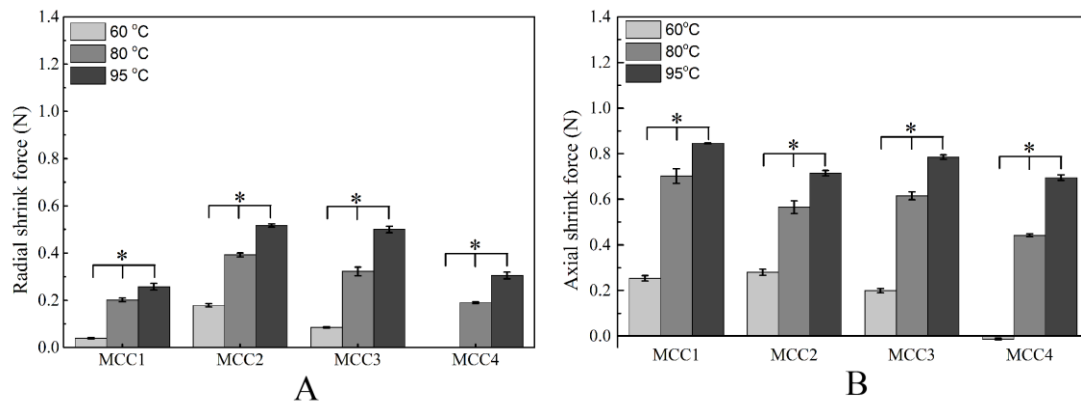


Fig. S6 The maximum radial (A,  $F_r$ ) and axial (B,  $F_a$ ) shrink force of MCCs in water at various temperatures (60 °C, 80 °C, 95 °C). The data are expressed as the means  $\pm$  SEM ( $n = 15$ ), \* denoted  $p < 0.05$ . Note: the  $F_a$  value of MCC4 at 60 °C appeared negative value, which were according to the expansion force due to the heating process.

Table S1 The protein and water content of various MCCs.

	MCC1	MCC2	MCC3	MCC4
Protein content (%)	61.74 $\pm$ 1.10	60.64 $\pm$ 0.96	61.58 $\pm$ 1.45	60.04 $\pm$ 1.37
Water content (%)	16.8 $\pm$ 0.25	16.19 $\pm$ 0.42	18.02 $\pm$ 0.32	17.70 $\pm$ 0.57